HHS Public Access

Author manuscript

Ultrasound Med Biol. Author manuscript; available in PMC 2022 April 01.

Published in final edited form as:

Ultrasound Med Biol. 2021 April ; 47(4): 1054–1066. doi:10.1016/j.ultrasmedbio.2020.12.024.

Time- and Dose-dependent Effects of Pulsed Ultrasound on Dermal Repair in Diabetic Mice

Melinda A. Vander Horst[a], **Carol H. Raeman**[a], **Diane Dalecki**[a], **Denise C. Hocking**[a,b,*]

[a]Department of Biomedical Engineering, University of Rochester, Rochester, New York 14642

[b]Department of Pharmacology and Physiology, University of Rochester, Rochester, New York 14642

Abstract

Chronic wounds, including diabetic, leg, and pressure ulcers, impose a significant health care burden worldwide. Some evidence indicates that ultrasound can enhance soft tissue repair. However, therapeutic responses vary among individuals, thereby limiting clinical translation. Here, effects of pulsed ultrasound on dermal wound healing were assessed using a murine model of chronic, diabetic wounds. An ultrasound exposure system was developed to provide daily ultrasound exposures to full-thickness, excisional wounds in genetically-diabetic mice. Wounds were exposed to 1-MHz ultrasound (2 ms pulse, 100 Hz PRF, 0-0.4 MPa) for 2 or 3 weeks. Granulation tissue thickness and wound re-epithelialization increased as a function of increasing ultrasound pressure amplitude. Two weeks after injury, significant increases in granulation tissue thickness and epithelial ingrowth were observed in response to 1-MHz pulsed ultrasound at 0.4 MPa. Wounds exposed to 0.4 MPa ultrasound for 3 weeks were characterized by collagen-dense, revascularized granulation tissue with a fully restored, mature epithelium. Of note, only half of wounds exposed to 0.4 MPa ultrasound showed significant granulation tissue deposition after 2 weeks of treatment. Thus, the *db+/db+* mouse model may help to identify biological variables that influence individual responses to pulsed ultrasound and accelerate clinical translation.

Keywords

therapeutic ultrasound; wound healing; chronic diabetic wounds; tissue regeneration

[*]**Address correspondence to:** Denise C. Hocking, Ph.D., Box 711, 601 Elmwood Ave., University of Rochester, Rochester, NY 14642, USA. Tel.: (585) 273-1770; FAX: (585) 273-2652; denise hocking@urmc.rochester.edu.

Declarations of Interest: none

Competing Interests
The authors declare that no competing interests exist.

INTRODUCTION

Chronic wounds have become a ‘silent epidemic’, affecting ~20 million people worldwide (Martinengo, et al. 2019), including more than 8 million Americans (Sen 2019). Non-healing wounds, which include diabetic, venous, and pressure ulcers, cause considerable pain and discomfort to the patient, with health complications ranging from serious infections to limb amputations to death. In the U.S., annual health care costs for treating chronic wounds are conservatively estimated at $32 billion (Nussbaum, et al. 2018). Diabetes, obesity, and aging are the major underlying causes of chronic wounds. According to a recent report from the Centers for Disease Control and Prevention (CDC 2020), over 30 million Americans, or 10.5% of the U.S. population, have been diagnosed with diabetes, while another 88 million Americans are pre-diabetic. Foot ulceration is the most common complication of diabetes; in the U.S., diabetic foot ulcers are the leading cause of non-traumatic lower extremity amputations, with an annual rate of 2 per 1000 adults with diabetes (Lin, et al. 2019). Current treatment approaches for chronic wounds include surgical debridement, moist dressings, engineered skin substitutes, compression therapy, negative pressure therapy, skin grafts, and recombinant growth factors. Yet, none of these approaches has proven to be an efficient and effective therapy, often yielding inconsistent results within identically treated populations for reasons that are not yet understood (Costa, et al. 2018, Frykberg and Banks 2015, Margolis, et al. 2013). Developing cost-effective treatment approaches that more consistently stimulate wound healing could greatly reduce healthcare and economic costs, lessen the chance of amputation, and improve the quality of life of patients with chronic wounds.

Ultrasound therapies that employ contact acoustic coupling have been investigated extensively as a treatment modality for cutaneous wounds. In vitro experiments using relatively low intensity (~0.05-0.5 W/cm^2), megahertz-frequency (~1-3 MHz) ultrasound indicate that ultrasound can stimulate cellular activities important to wound repair, including cell growth and proliferation (Doan, et al. 1999, Ramirez, et al. 1997, Samuels, et al. 2013, Zhou, et al. 2004), organized migration (Roper, et al. 2015), protein synthesis (Ramirez, et al. 1997, Webster, et al. 1980, Webster, et al. 1978), collagen deposition (Doan, et al. 1999), changes in membrane permeability (Dinno, et al. 1989, Mortimer and Dyson 1988), and growth factor release (Doan, et al. 1999, Ito, et al. 2000, Young and Dyson 1990). Conversely, other findings indicate that similar ultrasound exposures can lead to reduced cell growth or proliferation (Dyson, et al. 1968, Loch, et al. 1971).

Early work by the Dyson laboratory demonstrated that low intensity, megahertz-frequency, pulsed ultrasound could enhance soft tissue regeneration and remodeling in small animal models (Dyson, et al. 1970, Young and Dyson 1990, Young and Dyson 1990). Histological examination of tissues showed enhancement of protein synthesis but a temporary reduction in collagen bundles in wounds treated with ultrasound (Dyson, et al. 1970). Yet, studies investigating effects of low amplitude ultrasound on porcine wounds reported enhanced collagen deposition (Byl, et al. 1993, Byl, et al. 1992). Additional ultrasound-induced bioeffects observed in animal models of cutaneous wounds include increased angiogenesis (Young and Dyson 1990), inflammatory cell activity (Dyson and Luke 1986, Young and Dyson 1990), wound closure (Byl, et al. 1992, Roper, et al. 2015), vasodilation (Fischell, et

al. 1991, Hogan, et al. 1982, Suchkova, et al. 2000), and wound tensile strength (Byl, et al. 1993, Byl, et al. 1992).

Despite observations that ultrasound may accelerate wound healing in animal models, translation to the clinic has not yet been successful (Ennis, et al. 2016, Paliwal and Mitragotri 2008). Clinical investigations using megahertz-frequency, pulsed ultrasound have shown enhanced wound healing for venous or pressure ulcers (Dyson, et al. 1976, Polak, et al. 2016). However, other clinical studies have yielded contradictory results (Dyson, et al. 1976, Eriksson, et al. 1991, Lundeberg, et al. 1990, Watson, et al. 2011). More recent investigations of low-frequency ultrasound (20–30 kHz) suggest enhancement of wound healing in humans (Bajpai, et al. 2018, Peschen, et al. 1997, Polak, et al. 2016, Samuels, et al. 2013), though to-date, this effect has been observed only in small cohort studies.

In the present study, investigations were conducted to evaluate dose- and time-dependent effects of pulsed ultrasound on diabetic wound healing using a murine model of chronic dermal wounds. Genetically obese, leptin receptor-deficient mice (*db+/db+*) provide an animal model of impaired dermal wound healing that mirrors many of the clinical findings observed in patients with type II diabetes, including obesity, elevated plasma levels of glucose and insulin, and inflammation (Burke, et al. 2017, Galeano, et al. 2004, Luo, et al. 2004, Sullivan, et al. 2004). In response to 1-MHz, pulsed ultrasound, we identified differences in granulation tissue deposition, epithelial ingrowth and wound contraction as a function of ultrasound pressure amplitude. Notably, full thickness wounds exposed for 3 weeks to 1-MHz pulsed ultrasound at a pressure amplitude of 0.4 MPa were characterized by collagen-dense, revascularized granulation tissue with a fully restored, mature epithelium. However, our study also revealed marked intra-group variability in the responsiveness of young, male diabetic mice to ultrasound. To our knowledge, effects of pulsed ultrasound on dermal wounds in *db+/db+* mice mice have not been reported. Thus, these studies provide evidence that pulsed ultrasound can enhance repair of diabetic dermal wounds, and identify a novel murine model with which to investigate biological variables that influence individual responses to ultrasound.

MATERIALS AND METHODS

Animals

Male BKS.Cg-*Dock7*^{m}*+/+Lepr*^{db}/J mice (The Jackson Laboratories, Bar Harbor, ME) between ages 10-16 weeks were used for all studies. Mice were housed one per cage; water and laboratory chow were supplied *ad libitum*. Mice were weighed daily (MXX-612 Balance, Denver Instrument, Bohemia, NY) to monitor changes in health status. Blood glucose levels were measured weekly using blood from the tail vein of anesthetized mice and a TRUEtrack® Blood Glucose Monitoring System (Nipro Diagnostics, Fort Lauderdale, FL). Mice with blood glucose levels at or above 300 mg/dL were deemed diabetic (Matarese, et al. 2002, Roy, et al. 2013) and included in studies, whereas mice with blood glucose less than 300 mg/dL were omitted. All protocols were approved by the University Committee on Animal Resources at the University of Rochester.

Animal surgery

Three days prior to surgery, mice received acetaminophen (Major® Pharmaceuticals, Livonia, MI) at a final concentration of 0.3 mg/mL in water and Medigel® (ClearH20, Edwardsburg, MI) as required. Mice were anesthetized using either an injectable combination of ketamine (120 mg/kg; Hospira, Lake Forest, IL), xylazine (9.6 mg/kg; VEDCO, St. Joseph, MO) and buprenorphine (0.1 mg/kg; Par Pharmaceutical, Chestnut Ridge, NY), or sustained-release buphrenorphine (1 mg/kg; ZooPharm, Laramie, WY) with 2% isofluorane (MWI, Boise, ID) administered at a rate of 1 L/min oxygen. The different anesthesia methods had no significant intra-group effect on the healing outcomes of either sham or ultrasound-exposed wounds, as assessed by non-parametric Mann-Whitney tests (granulation tissue thickness, $P \geq 0.7$; epithelial ingrowth, $P \geq 0.1$; wound width, $P \geq 0.4$).

To produce full thickness dermal wounds, an area on the dorsal flank was shaved and depilated with Nair® (Princeton, NJ). On surgery day, mice were anesthetized, the shaved dorsal area was cleaned with iodide and 70% ethanol, and one full-thickness wound was made using a sterile 6-mm biopsy punch (Miltex, York, PA). A 15-μL volume of phosphate-buffered saline (PBS) was administered to the wound space and the wound was sealed with Tegaderm™ (3M Health Care). Mice were given saline (1 mL) subcutaneously to prevent dehydration. Animals continued to receive acetaminophen in their hydration sources until day 5 post-surgery.

Ultrasound exposures

The exposure system developed to deliver ultrasound to wounds is depicted in Fig. 1A. Ultrasound exposures were produced using a 1-MHz unfocused, single element, piezoceramic transducer. The transducer was affixed to a 3-axis positioner (Series B4000 Unislide; Velmex, Leatherhead, UK) and held in a stand-off filled with degassed and deionized water. A plastic, open-top mouse holder was placed in an exposure tank containing degassed and deionized water at 37 ° C. Acoustic windows (Saran wrap) were incorporated into the water standoff and plastic holder along the path of ultrasound transmission. Rubber absorbers were placed at the bottom of the water bath to limit acoustic reflections. Anesthetized mice were placed in the holder and the water standoff was coupled to Tegaderm™-covered wounds with Aquasonic® acoustic coupling gel (Parker Laboratories Inc., Fairfield NJ). The transducer was driven by a waveform generator (33120A; Hewlett Packard, Palo Alto, CA), attenuator (837; KayPENTAX, Montvale, NJ), and radio frequency power amplifier (2100 L; ENI, Rochester, NY). Acoustic fields were calibrated at the start and end of each experimental day under traveling wave conditions using a needle hydrophone (HNC-0400; Onda, Sunnyvale, CA). The distance between the transducer face and the wound was 2.6 cm.

Mice were randomly assigned to treatment conditions of 0, 0.1, 0.2, or 0.4 MPa, corresponding to I_{SPTA} values of 0, 0.05, 0.2, or 0.7 W/cm^2, respectively. All ultrasound treatments were administered at a frequency of 1 MHz, pulse repetition frequency of 100 Hz, and pulse duration of 2 ms. Exposure frequency and pulsing parameters were chosen to be similar to early work of Dyson (Dyson, et al. 1970, Young and Dyson 1990, Young and Dyson 1990), and pressure amplitudes were selected so as not to exceed relatively mild

ultrasound-induced heating for the highest amplitude tested. Mice received 2-min exposures at 4 overlapping sites around the wound periphery where wound closure originates (corresponding to 0° , 90° , 180° , and 270° , as depicted in Fig. 1B), for a total treatment time of 8 min. The −6 dB acoustic beam width was 7 mm. Thus, the entire Tegaderm-covered wound was exposed to ultrasound during treatment. Upon completion of the 8-min exposure, the Tegaderm™ dressing was removed, the wound was hydrated with PBS (15 μl), and new Tegaderm™ dressing was applied. Ultrasound exposures began within 5-10 min of wounding, and were then conducted daily, Monday-Friday, for either 2 or 3 weeks. No hair regrowth was observed during the 3-week treatment period. Sham-exposed (0 MPa) mice were subjected to identical procedures as ultrasound-exposed mice, but the transducer was not activated.

Temperature measurements

In separate studies, tissue temperature was measured during ultrasound exposure using wire type-T thermocouples. Punch biopsy wounds (6-mm diameter) were made on the dorsal flank of anaesthetized mice using protocols identical to those described above for wound healing studies. A thermocouple was placed at the wound edge, PBS (15 ¼l) was added to the wound, and the wound was covered using Tegaderm™. Mice were placed in the exposure tank and thermocouples were positioned at the beam center. To determine maximum potential tissue heating, wounds were exposed continuously for 8 min to 1-MHz pulsed ultrasound at a pressure amplitude of 0.4 MPa. Temperatures were recorded using a digital thermometer (BAT-12, Physitemp, Clifton, NJ).

Histological analysis

Mice were sacrificed on either day 14 or 21 after surgery. A 1 cm x 1 cm, full thickness segment of skin surrounding and including the wound space was excised from each mouse, fixed in 10% neutral buffered formalin, and paraffin-embedded for histological processing. Embedded tissue was cut into 6-μm-thick sections and mounted on glass microscope slides. Every tenth slide was stained with hematoxylin and eosin (H&E; MilliporeSigma, St. Louis, MO) to locate the center of the wound, which was identified as the section having the greatest distance between the severed edges of the dermal panniculus carnosus muscle. Slides immediately adjacent to the wound center were used for Masson’s trichrome staining (MilliporeSigma) or immunostaining.

For immunostaining, deparaffinized sections were processed for antigen retrieval by immersion in 0.01 M sodium citrate buffer, pH 6.0 at 60 °C for 1.5 h. Sections were treated with hydrogen peroxide to block endogenous peroxidase activity and then blocked with 3% bovine serum albumin (A3803, MilliporeSigma). Sections that were to be stained with anti-mouse primary antibodies were treated with Mouse-on-Mouse Blocking Reagent (Vector Laboratories, Burlingame, CA). Sections were incubated overnight at 4 °C with antibodies against α-smooth muscle actin (clone 1A4, MilliporeSigma; 1:1000) or filaggrin (clone Poly19058, Biolegend, San Diego, CA; 1:800), followed by species-matched, horseradish peroxidase-conjugated goat anti-rabbit or goat anti-mouse antibodies (Bio-Rad, Hercules, CA; 1:500). Bound antibodies were detected using 3,3′-diaminobenzidine (DAB) chromogen (Vector Laboratories, Burlingame, CA). Slides were counterstained with

hematoxylin. All sections were imaged using an inverted microscope (Olympus IX70; Center Valley, PA) equipped with a digital camera (MicroPublisher 3.3; Qlmaging, Surrey, British Columbia). The entire wound space was visualized by reconstructing overlapping images using Fiji (ImageJ software; NIH, Bethesda, MD).

Quantification of granulation tissue thickness, wound closure, re-epithelization, and wound width

Granulation tissue thickness, wound re-epithelization, and wound contraction were measured using H&E-stained tissue sections taken from the center of wounds. The center of each wound was identified by staining every 10th slide with H&E. Overlapping images of each tissue section were captured and stitched together using Fiji to produce a panoramic image that spanned the entire wound space. Wound widths of sequential sections were measured and the wound center was identified as the section having the maximum the wound width. Granulation tissue thickness was then measured at the midpoint of the wound using the severed ends of the panniculos carnosa muscle as markers of the wound edge. Granulation tissue was defined as the intact tissue within the wound space and excluded any epidermal regrowth.

Wound closure was determined from images of wounds obtained immediately after surgery (Day 0), before each ultrasound treatment, and before sacrifice on Day 14. Images were obtained following removal of the Tegaderm dressing using a Kodak Gel Logic 112 Imaging System and Carestream software (Kodak, Rochester, NY). Wound perimeters were traced using Carestream software to determine wound area. Wound areas are presented as a percentage of the ‘Day 0’ wound area, as described previously (Roy, et al. 2013).

Wound re-epithelization was determined by measuring epithelial ingrowth, defined as the distance between the original wound edge and the corresponding leading epithelial edge; data are presented as percent of original wound width. The original wound edges were identified in H&E-stained tissue sections using the corresponding severed edges of the dermal panniculus carnosus muscle as markers. Wounds were considered 100% re-epithelialized when a continuous epithelial layer spanned the wound space at the center of the wound.

To quantify wound width, the distance that remained between original wound edges at the center of the wound was measured. All histological quantifications were performed using Fiji. Investigators measuring tissue thickness, re-epithelization, and wound width were blinded to exposure conditions.

Statistical analysis

Data are expressed as mean ± standard error of the mean (SEM). Measures were compiled from at least 6 separate animals per exposure condition conducted over 3 separate experiments. Measurements of granulation tissue thickness, epithelial ingrowth, and wound width were analyzed using Grubbs’ test to identify outliers (GraphPad Prism, Version 8; LaJolla, CA). Animals were removed from the study if measurements of 2 of the above 3 wound healing parameters were identified as outliers. Using these criteria, 2 animals were removed from the 2-week study (1 sham-exposed mouse and 1 mouse exposed to 0.1 MPa).

No animals were removed from the 3-week study. After outlier removal, data distribution was analyzed using Anderson-Darling normality tests (GraphPad Prism), which indicated that granulation tissue thickness and epithelial ingrowth data at both time points were not normally distributed; data from these studies were analyzed using the Kruskal-Wallis test with Dunn's post-hoc test for multiple comparisons of groups (GraphPad Prism). Wound width data were normally distributed and analyzed using two-way analysis of variance (ANOVA) followed by Bonferroni's multiple comparison post-hoc tests (GraphPad Prism). *P* values less than 0.05 were considered significant. Data obtained from 2-week, sham-exposed mice (n=12) were used to compute 99% confidence intervals for granulation tissue thickness at the wound center. Linear regression analysis was performed using GraphPad Prism. Temperature measurements were conducted on 5 separate mice.

RESULTS

Ultrasound promotes granulation tissue deposition in diabetic mouse wounds

To investigate effects of pulsed ultrasound on full-thickness cutaneous wounds in an established murine model of diabetes, 6-mm-diameter punch biopsy wounds were made on the dorsal flank of genetically-diabetic, male mice. Wounds were exposed to ultrasound- or sham-treatment protocols, 5 days a week for either 2 or 3 weeks. A mild temperature increase of 2.6 ± 0.3 °C was observed at the wound edge in response to the highest pressure amplitude tested (0.4 MPa), resulting in a steady-state tissue temperature of 27.2 ± 0.7 °C at the center of the ultrasound beam during exposure. Upon completion of the 2- or 3-week treatment period, tissue sections from wound sites were harvested and granulation tissue deposition at the wound center was analyzed histologically to assess tissue regeneration independent of re-epithelialization. Fig. 2A shows representative H&E-stained tissue cross-sections obtained from the center of day 14 wounds. Two weeks after injury, sham-exposed wounds exhibited only a thin layer of new tissue in the wound space (Fig. 2A, 0 MPa), consistent with previous studies (Roy, et al. 2013). Similarly, wounds exposed to ultrasound at 0.1 MPa showed very little granulation tissue deposition (Fig. 2A). In contrast, dense granulation tissue was evident in wounds exposed to 1-MHz ultrasound at pressure amplitudes of 0.2 and 0.4 MPa (Fig. 2A). Average granulation tissue thickness increased as a function of increasing ultrasound pressure amplitude (Fig. 2B; R^2=0.93 by linear regression analysis). Additionally, treatment of wounds with ultrasound at 0.4 MPa resulted in a significant increase in granulation tissue thickness versus sham- (p=0.026) and 0.1 MPa-exposed wounds (p=0.017) (Fig. 2B).

The literature includes conflicting reports on the effectiveness of therapeutic ultrasound for soft tissue repair, and some populations exhibit a reduced response to therapeutic ultrasound (Alkahtani, et al. 2017, Robertson and Baker 2001). Thus, we next examined individual granulation tissue data points to assess individual responses to ultrasound treatments. Notably, the cohort of mice exposed to ultrasound at 0.4 MPa showed the possible presence of 2 distinct sub-populations (Fig. 3A). To determine if these data clusters were significantly different, statistical analyses were performed to determine the 99% confidence interval for granulation tissue thickness of sham-exposed wounds (n=12). Granulation tissue thickness measurements of 2-week, ultrasound-exposed wounds that were greater than the upper

boundary of this 99% confidence interval (i.e., >121 μm) were considered statistically different from sham and were classified as “responders” (Fig. 3A, red diamonds). Conversely, granulation tissue thickness values equal to or less than the upper boundary of the 99% confidence interval (i.e., ≤ 121 μm) were considered statistically similar to sham and designated “non-responders” (Fig. 3A, black circles). As shown in Fig. 3A, individual mice exposed to ultrasound at 0.4 MPa segregated into responder and non-responder clusters. Strikingly, average granulation tissue thickness of mice that responded to 0.4 MPa ultrasound was 594 ± 41 μm (n = 9), whereas average granulation tissue thickness of non-responders was 62 ± 25 μm (n = 10). Performing the same analysis with the other ultrasound treatment groups revealed that a similar proportion of mice responded to 0.2 (46%) and 0.4 MPa (47%) ultrasound, whereas only 18% of mice responded to 0.1 MPa ultrasound.

Digital images of wounds obtained from mice exposed to 0.4 MPa ultrasound were next analyzed to determine if wound closure rates also differed between responders and non-responders. As shown in Fig. 3B, graphs of wound closure rates of responders and non-responders began to show separation 3 days after wounding. Beginning on day 8 and continuing through day 14, significant differences in the extent of wound closure were observed between responders and non-responders (Fig. 3B), providing evidence that effects of ultrasound began within the first week of treatment.

Granulation tissue thickness was also measured after 3 weeks of exposure to ultrasound. Increased granulation tissue deposition was now evident in wounds exposed to 0.1 MPa compared to sham-exposed controls (Fig. 4A). As observed following 2 weeks of ultrasound exposure, granulation tissue thickness at 3 weeks increased as a function of ultrasound pressure amplitude (Fig. 4B; R^2=0.88 by linear regression analysis). After 3 weeks of ultrasound treatment with either 0.2 or 0.4 MPa ultrasound, granulation tissue thickness was approximately double that of sham-exposed wounds (0 MPa, 187 ± 56 μm; 0.2 MPa, 368 ± 44 μm; 0.4 MPa, 412 ± 85 μm). No significant differences were observed among treatment groups (Fig. 4B; p = 0.122 by Kruskal–Wallis test), Wound maturation was evident in wounds exposed to 0.2- and 0.4-MPa ultrasound, as numerous small blood vessels (Fig. 4A, arrows) and adipocytes (Fig. 4A, arrowheads) had repopulated the granulation tissue of those wounds. At the 3-week time point, continued gradual deposition of granulation tissue in sham-exposed wounds, occurring in parallel with maturation and contraction of wounds exposed to 0.2- and 0.4-MPa ultrasound, likely negated the differences in granulation tissue thickness observed at 2 weeks.

Increased wound contraction and collagen deposition of ultrasound-exposed wounds

Wound contraction typically begins towards the end of the proliferative stage of wound healing and is responsible for reducing the size of the defect (Falanga 2005). Wound contraction is critical for healing full-thickness injuries and is often impaired in chronic wounds (Falanga 2005). Here, wound contraction was assessed by measuring the distance between the edges of the original wound. After 2 weeks of treatment, no differences in wound width were observed among ultrasound- and sham-exposed wounds (Fig. 5A, ‘2 weeks’). Furthermore, no additional wound contraction occurred between 2 and 3 weeks in wounds exposed to either 0.1 MPa ultrasound or sham conditions (Fig. 5A). In contrast, the

widths of wounds exposed to ultrasound for 3 weeks at pressure amplitudes of either 0.2 or 0.4 MPa decreased significantly from the corresponding 2-week measurements, indicating that these wounds underwent significant contraction between the 2- and 3-week time points (Fig. 5A). Taken together, these results indicate that exposing wounds to 1-MHz ultrasound at pressure amplitudes of either 0.2 or 0.4 MPa for 3 weeks led to enhanced wound contraction.

To determine if the observed increase in wound contraction was accompanied by increased collagen density within the granulation tissue, tissue sections were stained with Masson's trichrome, which stains collagen blue. Granulation tissue of sham-exposed wounds showed only light collagen staining (Fig. 5B; 0 MPa). In contrast, collagen-dense granulation tissue that spanned the entire wound space was observed in wounds exposed to 1-MHz ultrasound at all pressure amplitudes (Fig. 5B). Notably, collagen staining was most dense at the center of wounds exposed at 0.4 MPa (Fig. 5B).

Ultrasound promotes re-epithelialization of diabetic mouse wounds

During normal wound repair, the formation of granulation tissue allows keratinocytes from surrounding healthy tissue to migrate into the wounded area to reestablish the epithelial barrier in a process termed re-epithelization. Wound re-epithelialization in response to 2- and 3-week ultrasound exposures was quantified by measuring the distance of epithelial migration across the wound space (Fig. 6A); values were expressed as a percentage of the measured wound width. After 2 weeks of exposure to 1-MHz ultrasound at 0.4 MPa, a significant increase in epithelial ingrowth was observed compared to sham- ($p = 0.006$) or 0.1 MPa- ($p = 0.022$) exposed wounds (Fig. 6B).

As with granulation tissue deposition, epithelial ingrowth increased between 2 and 3 weeks for all groups (Fig. 6C). Importantly, wounds of 12 of 13 mice (92%) exposed to ultrasound at either 0.2 or 0.4 MPa were fully re-epithelialized by week 3, compared to only 2 out of 6 mice (33%) in the sham-exposed group (Fig. 6D). Together, these data indicate that pulsed ultrasound promotes wound re-epithelization and that longer treatment times are associated with complete re-epithelialization of wounds.

Epidermal and granulation tissue maturation of ultrasound-exposed wounds

To further assess tissue maturation of ultrasound-exposed wounds, granulation tissue was evaluated for the presence of perfused blood vessels. To do so, tissue sections from 3-week, ultrasound- or sham-exposed wounds were stained with Masson's trichrome stain to identify red blood cells, or with anti-±SMA antibodies to identify vascular cells. In sham-exposed wounds, blood vessels were not evident at the center of the granulation tissue (Fig. 7A, E). In contrast, numerous blood vessels containing red blood cells were present at the center of the granulation tissue of wounds exposed at 0.1, 0.2, or 0.4 MPa (Fig. 7B–D, F–H), indicating the presence of a functional microvasculature within the newly deposited granulation tissue.

Mature epithelial layers that maintain effective barrier function require the presence of filaggrin, a protein responsible for aggregating keratins in the epidermis and a marker of late-stage epidermal differentiation (Sandilands, et al. 2009). To assess the maturity of the

epidermal layer of ultrasound-exposed wounds, tissue sections were stained for filaggrin. Sham-exposed, diabetic mouse wounds did not express filaggrin at the center of wounds 3 weeks after injury (Fig. 7I), consistent with the reduced level of re-epithelialization observed in this group (Fig. 6). In contrast, all re-epithelialized wounds that had been exposed to ultrasound at 0.1, 0.2, or 0.4 MPa showed strong and uninterrupted filaggrin expression across the wound (Fig. 7J–L), indicating a more advanced stage of wound healing compared to sham-exposed wounds.

Blood vessel density and epithelial maturation were also assessed at the inner wound edge of sham-exposed wounds and compared to corresponding regions of ultrasound-exposed wounds. Images obtained from the leading edge of sham-exposed wounds showed numerous clusters of small blood vessels (Fig. 8A, panels a and b) and a thickened, filaggrin-positive epithelium (Fig. 8A, panel c) compared to wounds exposed to 0.4 MPa ultrasound (Fig. 8A, panels d-f). The thickened epithelial tongue observed in sham-exposed wounds is consistent with the non-migratory, hyperproliferative epidermis that characterizes chronic wounds (Pastar, et al. 2014). No differences in tissue vascularization or epithelial filaggrin staining were observed in healthy tissue immediately adjacent to sham- (Fig. 8B, a–c) or ultrasound- (Fig. 8B, d–f) exposed wounds.

DISCUSSION

In this study, male, genetically diabetic mice were used to investigate effects of ultrasound pressure amplitude and treatment time on the healing of chronic dermal wounds. Chronic diabetic wounds in humans, including foot ulcers, are typically full-thickness injuries (Hunt 2011). Thus, as an experimental model, the full-thickness wound model provides clinical relevance as well as experimental value, as it exposes the wound bed to treatment and allows for histological analysis of the repair process throughout the epithelium and dermal tissues. Results of the present study showed that exposing full thickness, dermal wounds of diabetic mice to 1-MHz pulsed ultrasound increased granulation tissue deposition and re-epithelialization in a dose- and time-dependent manner. Wounds exposed to pulsed ultrasound (2 ms pulse, 100 Hz PRF) at 0.4 MPa (I_{SPTA} = 0.7 W/cm^2) for 8 min a day, 5 days a week for 2 weeks showed significantly more granulation tissue deposition (Fig. 2) and re-epithelization (Fig. 6) compared to sham-exposed wounds. Moreover, wounds exposed to pulsed ultrasound at 1 MHz and 0.4 MPa for 3 weeks were characterized by collagen-dense, contracted granulation tissue (Fig. 5), the presence of a functional microvasculature (Fig. 7), and a fully restored, differentiated epithelium (Fig. 7).

Diabetic wounds are characterized by both fibroblast and keratinocyte dysfunction, as well as reduced angiogenesis and neovasculation (Guo and Dipietro 2010). As such, our results provide evidence that 1-MHz pulsed ultrasound is a promising approach to accelerate wound repair and tissue regeneration of chronic, diabetic wounds. Pulsing parameters, frequency, and exposure amplitudes in our studies were comparable to the range of parameters tested in earlier work by Dyson (Dyson, et al. 1970, Young and Dyson 1990). Similar to Dyson et. al. (1970), in our studies, measured temperature increases due to ultrasound exposure were slight, thereby suggesting a non-thermal mechanism for effects of pulsed ultrasound on tissue healing and regeneration.

Complete wound healing is normally attained through a series of overlapping, temporally-related events that can be divided into 3 phases: inflammation, proliferation, and maturation (Guo and Dipietro 2010). The inflammatory phase begins with hemostasis and is characterized by recruitment of inflammatory cells to remove foreign debris and microbes (Guo and Dipietro 2010). Cytokines and growth factors released by inflammatory cells recruit stromal cells to the wound to initiate the proliferative phase, characterized by granulation tissue deposition and remodeling, re-epithelialization, and revascularization (Guo and Dipietro 2010). In turn, the maturational phase is marked by wound contraction, reduced cellularity and the formation of scar tissue (Reinke and Sorg 2012). In humans, the maturation phase starts approximately 3 weeks after injury and may last up to 12 months (Reinke and Sorg 2012). Wounds that do not heal in a timely manner or that do not possess sufficient mechanical strength are considered chronic (Guo and Dipietro 2010).

In the present study, sham-treated diabetic mouse wounds showed limited granulation tissue deposition at both 2 and 3 week timepoints (Figs. 2, 4), indicating that healing stalled in the inflammatory phase. In contrast, diabetic mouse wounds exposed for 3 weeks to ultrasound at 0.4 MPa had progressed to the proliferative phase of healing, as granulation tissue deposition, revascularization, and extensive re-epithelization were clearly evident in these wounds (Fig. 7). Increased collagen density and wound contraction were also observed after 3 weeks of ultrasound exposure at 0.4 MPa (Fig. 5), indicating that ultrasound-exposed wounds had progressed through the proliferative phase to the onset of the remodeling phase. It is not known whether the additional week of ultrasound treatment contributed directly to the healing response, or whether 2 weeks of ultrasound exposure followed by an additional week of healing would provide similar therapeutic benefits. Significant differences in the extent of wound closure were observed between responders and non-responders following the first week of ultrasound treatment (Fig. 3B), providing evidence that effects of ultrasound were inititated in the inflammatory and early proliferative stages of wound healing. Together, these results indicate that pulsed ultrasound treatment can advance chronic diabetic wounds from a stalled inflammatory phase through the proliferative phase of wound healing, and are in agreement with previous work indicating that ultrasound accelerates the inflammatory and early proliferative stages of repair (Dyson and Luke 1986, Young and Dyson 1990).

The cellular targets of pulsed ultrasound therapy are unknown. In granulation tissue, collagen deposition and remodeling are key functions of fibroblasts (Reinke and Sorg 2012). In the current study, collagen deposition was increased throughout wounds exposed to ultrasound, with dense collagen staining observed in wounds exposed at 0.4 MPa, consistent with reports that ultrasound enhances collagen deposition in porcine wounds (Byl, et al. 1993, Byl, et al. 1992). Additionally, increased wound contraction was observed after 3 weeks of treatment with either 0.2 or 0.4 MPa ultrasound. Myofibroblast-mediated remodeling of collagen fibrils is responsible for wound contraction (Reinke and Sorg 2012). Together, these data indicate a return to normal fibroblast function with ultrasound treatment.

During skin formation, properly timed keratinocyte differentiation and cell death are essential for the formation of the outer epidermal layer which is responsible for protecting

against physical injury, water loss, and infection (Brown and McLean 2012, Sandilands, et al. 2009). During keratinocyte differentiation, cells withdraw from the cell cycle, move to an outer epidermal layer and undergo a type of programmed death called cornification (Eckhart, et al. 2013, Sandilands, et al. 2009). Filaggrin production by keratinocytes triggers differentiation, slows proliferation, and allows cell cycle arrest to be timed appropriately for widespread cornification (Aho, et al. 2012, Gutowska-Owsiak, et al. 2018, Presland, et al. 2001). Non-healing ulcers often express very low levels of filaggrin (Stojadinovic, et al. 2008). Loss of filaggrin has been associated with keratinocyte dysfunction, impaired keratinization, and defective barrier function (Kawasaki, et al. 2012, Pendaries, et al. 2014, Smith, et al. 2006). Thus, the observation that epithelial filaggrin is expressed in ultrasound-exposed wounds (Fig. 7) indicates that keratinocytes are not only present at the center of the wound, but that they are functional, going through late-stage differentiation and in the process of forming a cornified layer.

The literature contains a history of conflicting reports on the effectiveness of ultrasound for soft tissue wound repair, and certain populations do not respond to therapeutic ultrasound (Alkahtani, et al. 2017, Qaseem, et al. 2015, Robertson and Baker 2001, Smith, et al. 2013, ter Riet, et al. 1996). Interestingly, not all mice exposed to ultrasound progressed through the first 2 phases of healing at similar rates, as granulation tissue thickness of more than half of the mice exposed to ultrasound at 0.4 MPa for 2 weeks was not different from sham-exposed wounds (Fig. 3A). The biologic and/or acoustic factors that may have contributed to the varied sensitivity of individual mice to ultrasound treatment are currently unknown. We found no differences between responder and non-responder groups in either body weight (in g: sham, 44.89 ±1.4; responders, 43.22 ± 1.6; non-responders, 41.5 ±1.7; $p > 0.05$ by ANOVA) or blood glucose levels (in mg/dl: sham, 709.5 ± 41.5; responders, 620 ± 45.1; non-responders, 736 ± 68.3; $p > 0.05$ by ANOVA). As well, no differences in collagen content, tissue thickness, or adipose levels were observed in uninjured skin distant from the wound in responders versus non-responders (not shown). Identifying key factors that influence tissue responsivenes to ultrasound would allow for clinicians to tailor ultrasound treatment protocols for individual patients for increased therapeutic success. As such, the *db+/db+* mouse model may serve as an important new tool for identifying biological variables that influence responses to pulsed ultrasound.

In summary, in response to daily, 8-min treatments with 1-MHz, pulsed ultrasound, full thickness dermal wounds of diabetic mice showed increased granulation tissue deposition, epithelial ingrowth, and wound contraction as a function of ultrasound pressure amplitude and the number of treatment weeks. Our study also revealed intra-group variability in the responsiveness of young, obese, male diabetic mice to pulsed ultrasound after 2 weeks of treatment. Full thickness wounds exposed for 3 weeks to 1-MHz pulsed ultrasound at a pressure amplitude of 0.4 MPa were characterized by collagen-dense, revascularized granulation tissue and a fully restored, mature epithelium. Taken together, these results provide evidence that treatment of chronic, diabetic wounds with 1-MHz pulsed ultrasound can stimulate wound repair, and identify a murine model that may serve to uncover biological variables that influence individual responses to ultrasound.

Acknowledgments

Funding

This research was supported by National Institutes of Health (NIH) Grant R01AG058746.

REFERENCES

Aho S, Harding CR, Lee J-M, Meldrum H, Bosko CA. Regulatory role for the profilaggrin N-terminal domain in epidermal homeostasis. J. Invest. Dermatol 2012; 132:2376–85. [PubMed: 22622429]

Alkahtani SA, Kunwar PS, Jalilifar M, Rashidi S, Yadollahpour A. Ultrasound-based Techniques as Alternative Treatments for Chronic Wounds: A Comprehensive Review of Clinical Applications. Cureus 2017; 9:e1952. [PubMed: 29487767]

Bajpai A, Nadkarni S, Neidrauer M, Weingarten MS, Lewin PA, Spiller KL. Effects of non-thermal, non-cavitational ultrasound exposure on human diabetic ulcer healing and inflammatory gene expression in a pilot study. Ultrasound in Medicine & Biology 2018; 44:2043–49. [PubMed: 29941215]

Brown SJ, McLean WI. One remarkable molecule: filaggrin. J. Invest. Dermatol 2012; 132:751–62. [PubMed: 22158554]

Burke SJ, Batdorf HM, Burk DH, Noland RC, Eder AE, Boulos MS, Karlstad MD, Collier JJ. db/db Mice Exhibit Features of Human Type 2 Diabetes That Are Not Present in Weight-Matched C57BL/6J Mice Fed a Western Diet. J Diabetes Res 2017; 2017:8503754. [PubMed: 29038790]

Byl NN, McKenzie A, Wong T, West J, Hunt TK. Incisional wound healing: a controlled study of low and high dose ultrasound. Journal of Orthopaedic & Sports Physical Therapy 1993; 18:619–28.

Byl NN, McKenzie AL, West JM, Whitney JD, Hunt TK, Scheuenstuhl HA. Low-dose ultrasound effects on wound healing: a controlled study with Yucatan pigs. Arch. Phys. Med. Rehabil 1992; 73:656–64. [PubMed: 1622322]

CDC. 2020 National Diabetes Statistics Report 2020: Estimates of Diabetes and its Burden in the United States.

Costa ML, Achten J, Bruce J, Tutton E, Petrou S, Lamb SE, Parsons NR. Effect of negative pressure wound therapy vs standard wound management on 12-month disability among adults with severe open fracture of the lower limb: The WOLLF randomized clinical trial. Journal of the American Medical Association 2018; 319:2280–88. [PubMed: 29896626]

Dinno M, Dyson M, Young S, Mortimer A, Hart J, Crum L. The significance of membrane changes in the safe and effective use of therapeutic and diagnostic ultrasound. Physics in Medicine and Biology 1989; 34:1543. [PubMed: 2685832]

Doan N, Reher P, Meghji S, Harris M. In vitro effects of therapeutic ultrasound on cell proliferation, protein synthesis, and cytokine production by human fibroblasts, osteoblasts, and monocytes. J. Oral Maxillofac. Surg 1999; 57:409–19. [PubMed: 10199493]

Dyson M, Franks C, Suckling J. Stimulation of healing of varicose ulcers by ultrasound. Ultrasonics 1976; 14:232–36. [PubMed: 973258]

Dyson M, Luke DA. Induction of mast cell degranulation in skin by ultrasound. IEEE Transactions on Ultrasonics, Ferroelectrics, and Frequency Control 1986; 33:194–201.

Dyson M, Pond JB, Joseph J, Warwick R. The stimulation of tissue regeneration by means of ultrasound. Clin. Sci 1968; 35:273. [PubMed: 5721232]

Dyson M, Pond JB, Joseph J, Warwick R. Stimulation of tissue regeneration by pulsed plane-wave ultrasound. IEEE Transactions on Sonics and Ultrasonics 1970; 17:133–39.

Eckhart L, Lippens S, Tschachler E, Declercq W. Cell death by cornification. Biochimica et Biophysica Acta (BBA)-Molecular Cell Research 2013; 1833:3471–80. [PubMed: 23792051]

Ennis WJ, Lee C, Gellada K, Corbiere TF, Koh TJ. Advanced Technologies to Improve Wound Healing: Electrical Stimulation, Vibration Therapy, and Ultrasound-What Is the Evidence? Plastic Reconstructive Surgery 2016; 138:94S–104S. [PubMed: 27556780]

Eriksson SV, Lundebergz T, Malrn M. A placebo controlled trial of ultrasound therapy in chronic leg ulceration. Allergy 1991; 2:3.

Falanga V Wound healing and its impairment in the diabetic foot. The Lancet 2005; 366:1736–43.

Fischell TA, Abbas MA, Grant GW, Siegel RJ. Ultrasonic energy. Effects on vascular function and integrity. Circulation 1991; 84:1783–95. [PubMed: 1914114]

Frykberg RG, Banks J. Challenges in the treatment of chronic wounds. Adv. Wound Care 2015; 4:560–82.

Galeano M, Altavilla D, Cucinotta D, Russo GT, Calo M, Bitto A, Marini H, Marini R, Adamo EB, Seminara P. Recombinant human erythropoietin stimulates angiogenesis and wound healing in the genetically diabetic mouse. Diabetes 2004; 53:2509–17. [PubMed: 15331568]

Guo S, Dipietro LA. Factors affecting wound healing. Journal of Dental Research 2010; 89:219–29. [PubMed: 20139336]

Gutowska-Owsiak D, de La Serna JB, Fritzsche M, Naeem A, Podobas El, Leeming M, Colin-York H, O'Shaughnessy R, Eggeling C, Ogg GS. Orchestrated control of filaggrin–actin scaffolds underpins cornification. Cell Death Dis. 2018; 9:1–18. [PubMed: 29298988]

Hogan R, Franklin T, Fry F, Avery K, Burke K. The effect of ultrasound on microvascular hemodynamics in skeletal muscle: effect on arterioles. Ultrasound in Medicine & Biology 1982; 8:45–55.

Hunt DL. Diabetes: foot ulcers and amputations. BMJ Clin Evid 2011; 2011.

Ito M, Azuma Y, Ohta T, Komoriya K. Effects of ultrasound and 1, 25-dihydroxyvitamin D3 on growth factor secretion in co-cultures of osteoblasts and endothelial cells. Ultrasound in Medicine & Biology 2000; 26:161–66. [PubMed: 10687804]

Kawasaki H, Nagao K, Kubo A, Hata T, Shimizu A, Mizuno H, Yamada T, Amagai M. Altered stratum corneum barrier and enhanced percutaneous immune responses in filaggrin-null mice. J. Allergy Clin. Immunol 2012; 129:1538–46. e6. [PubMed: 22409988]

Lin CW, Armstrong DG, Lin CH, Liu PH, Hung SY, Lee SR, Huang CH, Huang YY. Nationwide trends in the epidemiology of diabetic foot complications and lower-extremity amputation over an 8-year period. BMJ Open Diabetes Research Care 2019; 7:e000795.

Loch E, Fischer A, Kuwert E. Effect of diagnostic and therapeutic intensities of ultrasonics on normal and malignant human cells in vitro. American Journal of Obstetrics and Gynecology 1971; 110:457–60. [PubMed: 5582000]

Lundeberg T, Nordström F, Brodda-Jansen G, Eriksson S, Kjartansson J, Samuelson U. Pulsed ultrasound does not improve healing of venous ulcers. Scandinavian Journal of Rehabilitation Medicine 1990; 22:195–97. [PubMed: 2263919]

Luo J-D, Wang Y-Y, Fu W-L, Wu J, Chen AF. Gene therapy of endothelial nitric oxide synthase and manganese superoxide dismutase restores delayed wound healing in type 1 diabetic mice. Circulation 2004; 110:2484–93. [PubMed: 15262829]

Margolis DJ, Gupta J, Hoffstad O, Papdopoulos M, Glick HA, Thom SR, Mitra N. Lack of effectiveness of hyperbaric oxygen therapy for the treatment of diabetic foot ulcer and the prevention of amputation: a cohort study. Diabetes Care 2013:DC_122160.

Martinengo L, Olsson M, Bajpai R, Soljak M, Upton Z, Schmidtchen A, Car J, Jarbrink K. Prevalence of chronic wounds in the general population: systematic review and meta-analysis of observational studies. Annals Epidemiology 2019; 29:8–15.

Matarese G, Sanna V, Lechler RI, Sarvetnick N, Fontana S, Zappacosta S, La Cava A. Leptin accelerates autoimmune diabetes in female NOD mice. Diabetes 2002; 51:1356–61. [PubMed: 11978630]

Mortimer A, Dyson M. The effect of therapeutic ultrasound on calcium uptake in fibroblasts. Ultrasound in Medicine & Biology 1988; 14:499–506. [PubMed: 3227573]

Nussbaum SR, Carter MJ, Fife CE, DaVanzo J, Haught R, Nusgart M, Cartwright D. An Economic Evaluation of the Impact, Cost, and Medicare Policy Implications of Chronic Nonhealing Wounds. Value Health 2018; 21:27–32. [PubMed: 29304937]

Paliwal S, Mitragotri S. Therapeutic opportunities in biological responses of ultrasound. Ultrasonics 2008; 48:271–8. [PubMed: 18406440]

Pastar I, Stojadinovic O, Yin NC, Ramirez H, Nusbaum AG, Sawaya A, Patel SB, Khalid L, Isseroff RR, Tomic-Canic M. Epithelialization in Wound Healing: A Comprehensive Review. Adv Wound Care (New Rochelle) 2014; 3:445–64. [PubMed: 25032064]

Pendaries V, Malaisse J, Pellerin L, Le Lamer M, Nachat R, Kezic S, Schmitt A-M, Paul C, Poumay Y, Serre G. Knockdown of filaggrin in a three-dimensional reconstructed human epidermis impairs keratinocyte differentiation. J. Invest. Dermatol 2014; 134:2938–46. [PubMed: 24940654]

Peschen M, Weichenthal M, Schöpf E, Vanscheidt W. Low-frequency ultrasound treatment of chronic venous leg ulcers in an outpatient therapy. Acta dermato-venereologica 1997; 77:311–14. [PubMed: 9228227]

Polak A, Taradaj J, Nawrat-Szoltysik A, Stania M, Dolibog P, Blaszczak E, Zarzeczny R, Juras G, Franek A, Kucio C. Reduction of pressure ulcer size with high-voltage pulsed current and high-frequency ultrasound: a randomised trial. J. Wound Care 2016; 25:742–54. [PubMed: 27974012]

Presland RB, Kuechle MK, Lewis SP, Fleckman P, Dale BA. Regulated expression of human filaggrin in keratinocytes results in cytoskeletal disruption, loss of cell–cell adhesion, and cell cycle arrest. Exp. Cell Res 2001; 270:199–213. [PubMed: 11640884]

Qaseem A, Humphrey LL, Forciea MA, Starkey M, Denberg TD. Treatment of pressure ulcers: a clinical practice guideline from the American College of Physicians. Ann. Intern. Med 2015; 162:370–79. [PubMed: 25732279]

Ramirez A, Schwane JA, McFARLAND C, Starcher B. The effect of ultrasound on collagen synthesis and fibroblast proliferationin vitro. Medicine & Science in Sports & Exercise 1997; 29:326–32. [PubMed: 9139171]

Reinke JM, Sorg H. Wound repair and regeneration. Eur. Surg. Res 2012; 49:35–43. [PubMed: 22797712]

Robertson VJ, Baker KG. A review of therapeutic ultrasound: effectiveness studies. Physical Therapy 2001; 81:1339–50. [PubMed: 11444997]

Roper JA, Williamson RC, Bally B, Cowell CA, Brooks R, Stephens P, Harrison AJ, Bass MD. Ultrasonic stimulation of mouse skin reverses the healing delays in diabetes and aging by activation of Rac1. J. Invest. Dermatol 2015; 135:2842–51. [PubMed: 26079528]

Roy DC, Mooney NA, Raeman CH, Dalecki D, Hocking DC. Fibronectin matrix mimetics promote full-thickness wound repair in diabetic mice. Tissue Engineering Part A 2013; 19:2517–26. [PubMed: 23808793]

Samuels JA, Weingarten MS, Margolis DJ, Zubkov L, Sunny Y, Bawiec CR, Conover D, Lewin PA. Low-frequency (< 100 kHz), low-intensity (< 100 mW/cm2) ultrasound to treat venous ulcers: A human study and in vitro experiments. The Journal of the Acoustical Society of America 2013; 134:1541–47. [PubMed: 23927194]

Sandilands A, Sutherland C, Irvine AD, McLean Wl. Filaggrin in the frontline: role in skin barrier function and disease. Journal of Cell Science 2009; 122:1285–94. [PubMed: 19386895]

Sen CK. Human Wounds and Its Burden: An Updated Compendium of Estimates. Adv Wound Care (New Rochelle) 2019; 8:39–48. [PubMed: 30809421]

Smith FJ, Irvine AD, Terron-Kwiatkowski A, Sandilands A, Campbell LE, Zhao Y, Liao H, Evans AT, Goudie DR, Lewis-Jones S. Loss-of-function mutations in the gene encoding filaggrin cause ichthyosis vulgaris. Nat. Genet 2006; 38:337–42. [PubMed: 16444271]

Smith ME, Totten A, Hickam DH, Fu R, Wasson N, Rahman B, Motu'apuaka M, Saha S. Pressure ulcer treatment strategies: a systematic comparative effectiveness review. Ann Intern Med 2013; 159:39–50. [PubMed: 23817703]

Stojadinovic O, Pastar I, Vukelic S, Mahoney MG, Brennan D, Krzyzanowska A, Golinko M, Brem H, Tomic-Canic M. Deregulation of keratinocyte differentiation and activation: a hallmark of venous ulcers. J. Cell. Mol. Med 2008; 12:2675–90. [PubMed: 18373736]

Suchkova V, Baggs R, Francis C. Effect of 40-kHz ultrasound on acute thrombotic ischemia in a rabbit femoral artery thrombosis model: enhancement of thrombolysis and improvement in capillary muscle perfusion. Circulation 2000; 101:2296–301. [PubMed: 10811598]

Sullivan SR, Underwood RA, Gibran NS, Sigle RO, Usui ML, Carter WG, Olerud JE. Validation of a model for the study of multiple wounds in the diabetic mouse (db/db). Plast Reconstr Surg 2004; 113:953–60. [PubMed: 15108888]

ter Riet G, Kessels AG, Knipschild P. A randomized clinical trial of ultrasound in the treatment of pressure ulcers. Physical Therapy 1996; 76:1301–12. [PubMed: 8959999]

Watson JM, Kang'ombe AR, Soares MO, Chuang LH, Worthy G, Bland JM, Iglesias C, Cullum N, Torgerson D, Nelson EA, Ven USIllt. Ven US III: a randomised controlled trial of therapeutic ultrasound in the management of venous leg ulcers. Health Technol. Assess 2011; 15:1–192.

Webster D, Harvey W, Dyson M, Pond J. The role of ultrasound-induced cavitation in the 'in vitro'stimulation of collagen synthesis in human fibroblasts. Ultrasonics 1980; 18:33–37. [PubMed: 7350723]

Webster D, Pond J, Dyson M, Harvey W. The role of cavitation in the in vitro stimulation of protein synthesis in human fibroblasts by ultrasound. Ultrasound in Medicine & Biology 1978; 4:343–51. [PubMed: 753008]

Young S, Dyson M. The effect of therapeutic ultrasound on angiogenesis. Ultrasound Med. Biol 1990; 16:261–69. [PubMed: 1694604]

Young S, Dyson M. Effect of therapeutic ultrasound on the healing of full-thickness excised skin lesions. Ultrasonics 1990; 28:175–80. [PubMed: 2339476]

Young S, Dyson M. Macrophage responsiveness to therapeutic ultrasound. Ultrasound in Medicine & Biology 1990; 16:809–16. [PubMed: 2095011]

Zhou S, Schmelz A, Seufferlein T, Li Y, Zhao J, Bachem MG. Molecular mechanisms of low intensity pulsed ultrasound in human skin fibroblasts. J. Biol. Chem 2004; 279:54463–69. [PubMed: 15485877]

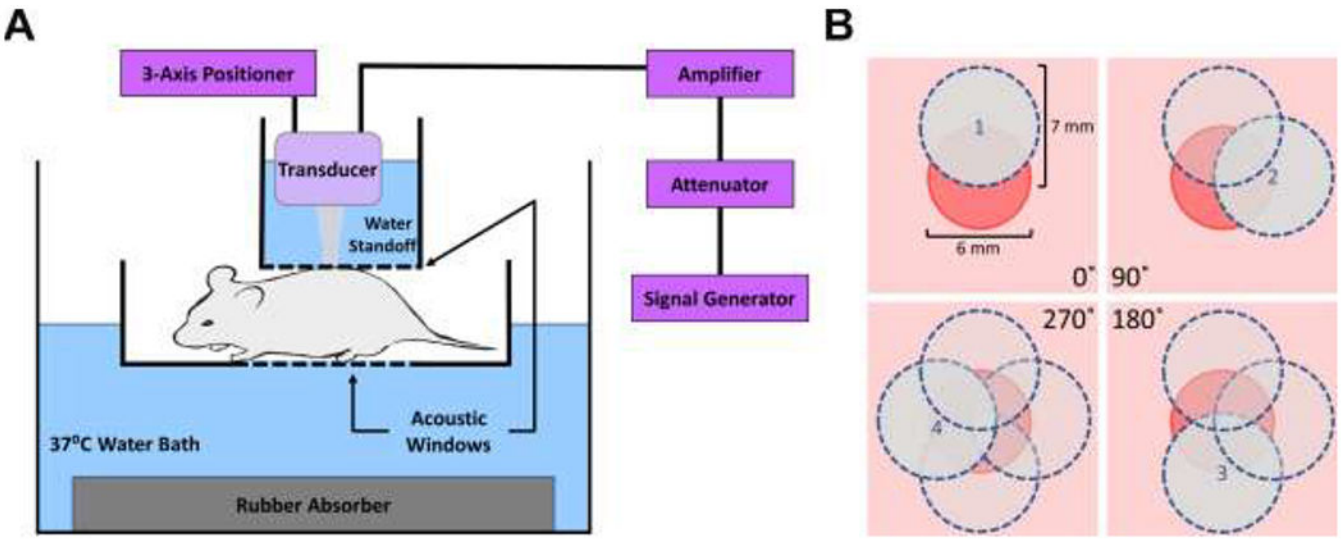

Fig. 1. Schematic of ultrasound exposure system and protocol

(A) Anesthetized mice were placed in a plastic holder that was partially submerged in an exposure tank filled with degassed and deionized water. A water standoff was coupled to the wound with acoustic coupling gel and an acoustic absorber was used to limit reflections. A 1-MHz, unfocused ultrasound transducer was located within the water standoff using a three-axis positioner. (B) Depiction of a 6-mm punch biopsy wound (red circle) as viewed from above. On each treatment day, 4 overlapping sites around the wound periphery were exposed to ultrasound for 2 min each, for a total exposure time of 8 min. The area of the 7 mm-diameter, −6 dB beam width of each exposure (blue circles) collectively covered the entire wound area.

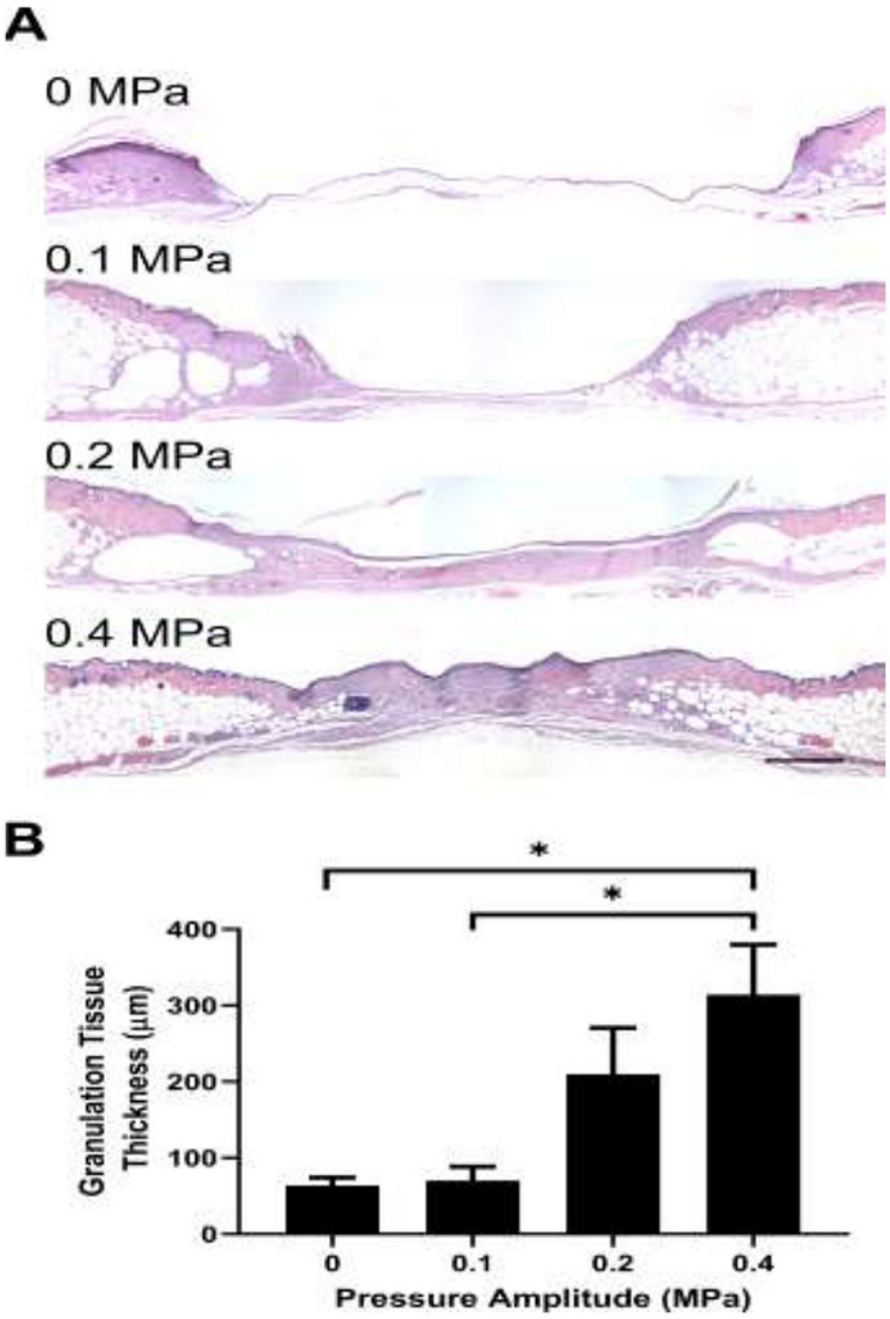

Fig. 2. Effects of pulsed ultrasound on granulation tissue deposition two weeks after injury

Full thickness punch biopsy wounds were either sham-exposed or exposed to 1-MHz, pulsed ultrasound at pressure amplitudes of 0.1, 0.2, or 0.4 MPa for 2 weeks. Fourteen days after injury, animals were sacrificed, and wounds were excised and processed for histology. (A) H&E-stained skin sections from the center of wounds exposed at 0, 0.1, 0.2 or 0.4 MPa ultrasound. Images represent average granulation tissue thickness values from each group. Scale bar = 500 μm. (B) Granulation tissue thickness was measured at the wound center and plotted as an average for each treatment condition (n = 11-19). * $p < 0.05$ using the Kruskal–

Wallis test with Dunn's post-hoc test. Significant differences found between 0.4 MPa and 0 MPa ($p = 0.026$) as well as 0.4 MPa and 0.1 MPa ($p = 0.017$). Error bars indicate SEM.

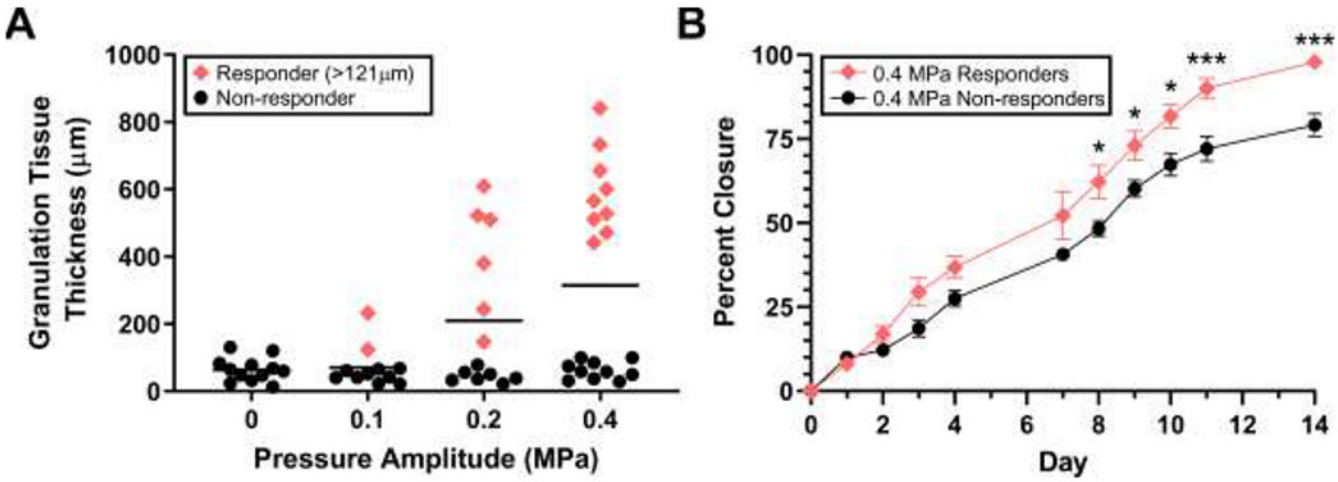

Fig. 3. Individual variability in the response to ultrasound

(A) Individual granulation tissue values from the 2-week study were plotted as a function of pressure amplitude. Values from ultrasound-exposed mice that were statistically different from sham were determined by establishing a 99% confidence interval of time-matched, sham-exposed mice (n = 12). Data points greater than the upper bound of the 99% confidence interval (> 121 μm) were categorized as responders (red diamonds). Values less than or equal to the 99% confidence interval were considered non-responders (black circles). Bars represent mean values. (B) Diabetic mouse wounds treated with 1-MHz, 0.4-MPa ultrasound were imaged immediately after surgery (Day 0), before ultrasound treatment on each subsequent day, and before sacrifice on day 14. Average percent closure of "responders" (n = 9) and "non-responders" (n = 10) was plotted over time (± SEM). Significant differences between responder and non-responder groups were determined by 2-way ANOVA and Bonferroni's multiple comparison testing (*$p < 0.05$, ***$p < 0.001$). Significant differences between responders and non-responders were found on day 8 ($p = 0.017$), 9 ($p = 0.036$), 10 ($p = 0.013$), 11 ($p < 0.001$), and 14 ($p < 0.001$).

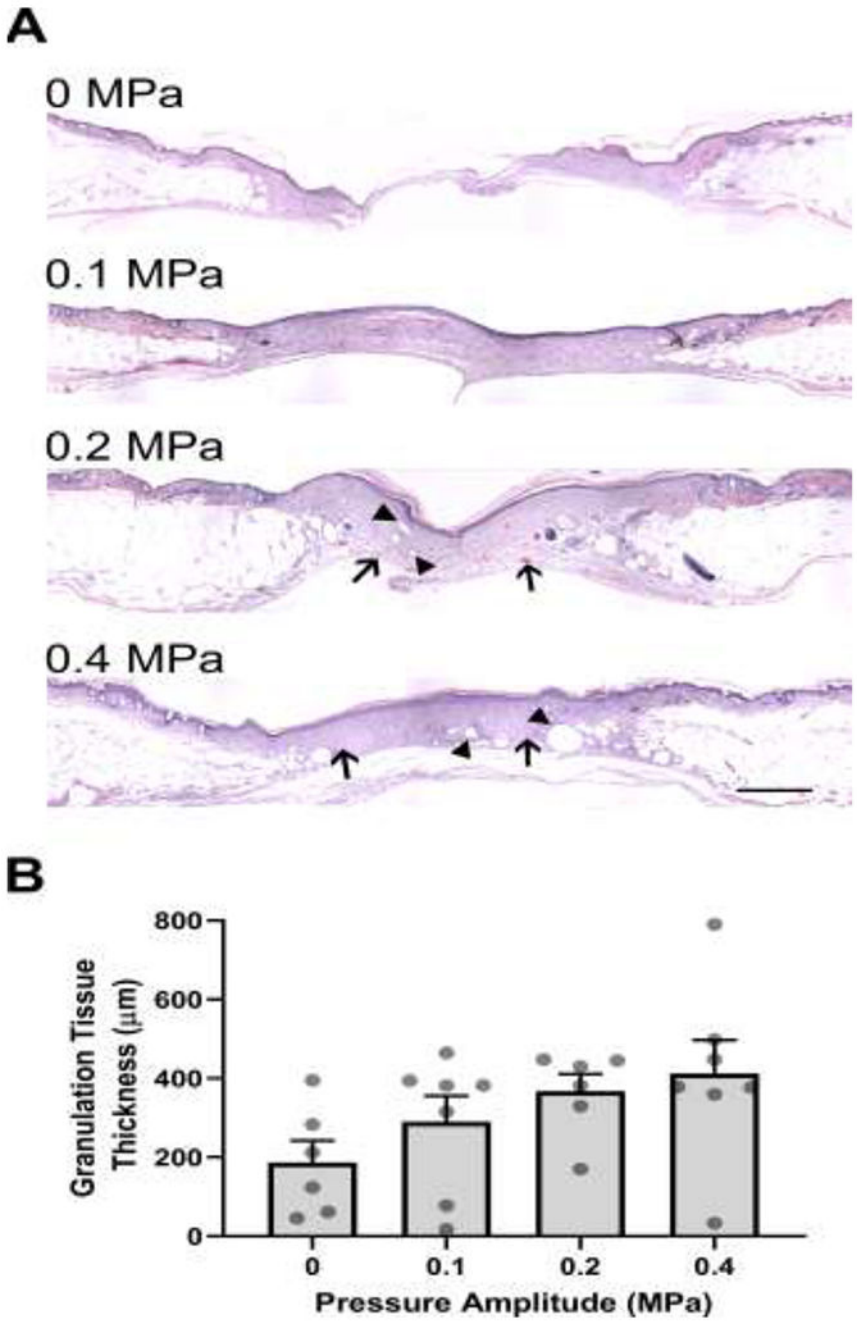

Fig. 4. Quantification of granulation tissue deposition in diabetic wounds after 3 weeks of ultrasound treatment

Full-thickness, diabetic mouse wounds were exposed to 1-MHz pulsed ultrasound at 0, 0.1, 0.2, or 0.4 MPa for 3 weeks. Three weeks after injury, mice were sacrificed, and their wound tissue harvested. (A) H&E-stained skin sections from the center of wounds. Images represent average granulation tissue thickness values from each group. Scale bar = 500 μm. (B) Granulation tissue thicknesses at the center of the wounds were quantified (n = 6-7). Graph shows individual data points representing the granulation tissue thickness of each

animal, bars represent mean values for each treatment condition, and error bars indicate SEM.

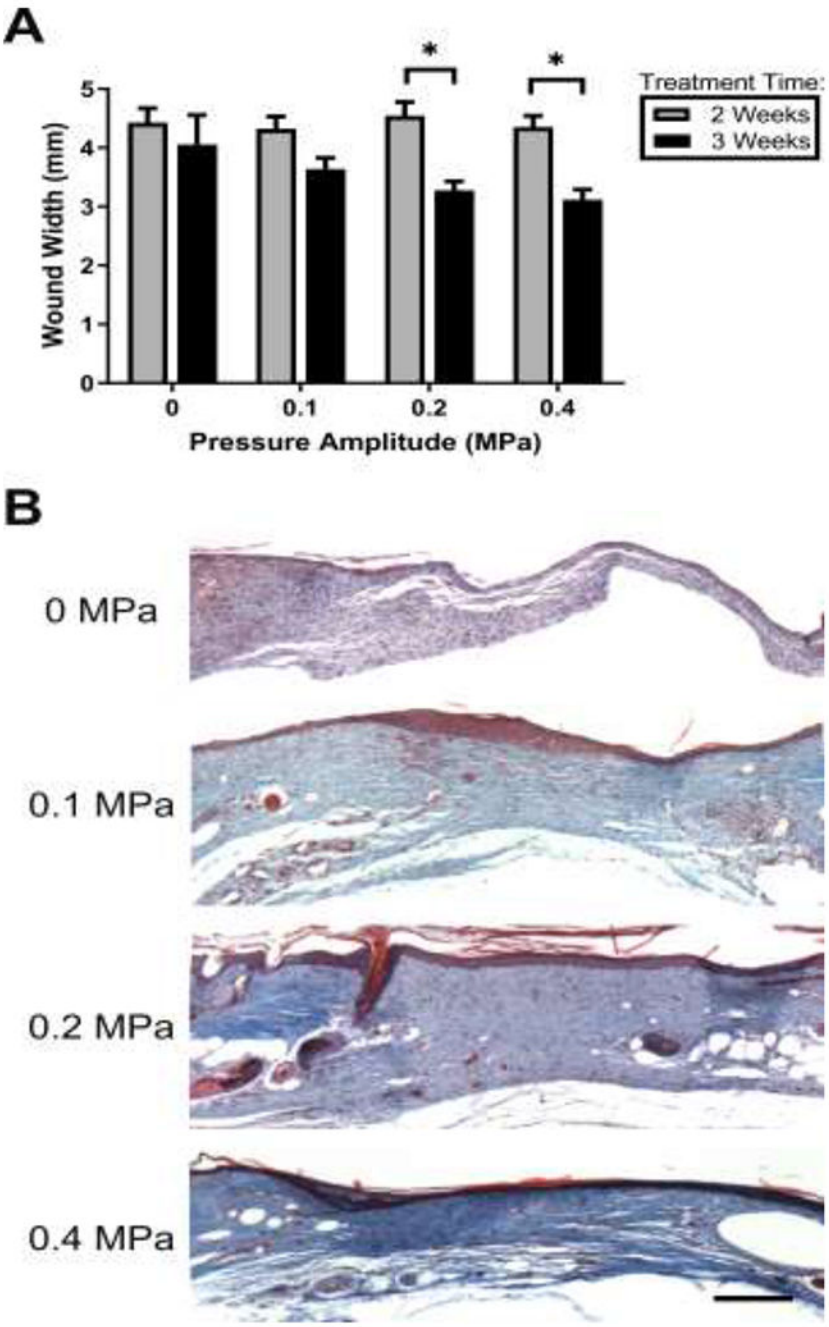

Fig. 5. Effects of ultrasound on wound contraction and collagen deposition

(A) Wound widths were determined by measuring the distance between the severed edges of the panniculus carnosus muscle layer using H&E-stained tissue sections from the center of each wound. $^{**}p < 0.01$; 2-way ANOVA and Bonferroni's multiple comparison post-hoc test. 2- and 3-week treatments were significantly different from one another at 0.2 and 0.4 MPa pressure amplitudes ($p = 0.006$ and $p = 0.003$, respectively). (B) Representative images of Masson's trichrome-stained sections from the center of wounds exposed to pulsed ultrasound at 0, 0.1, 0.2, or 0.4 MPa for 3 weeks. Scale bar = 200 μm.

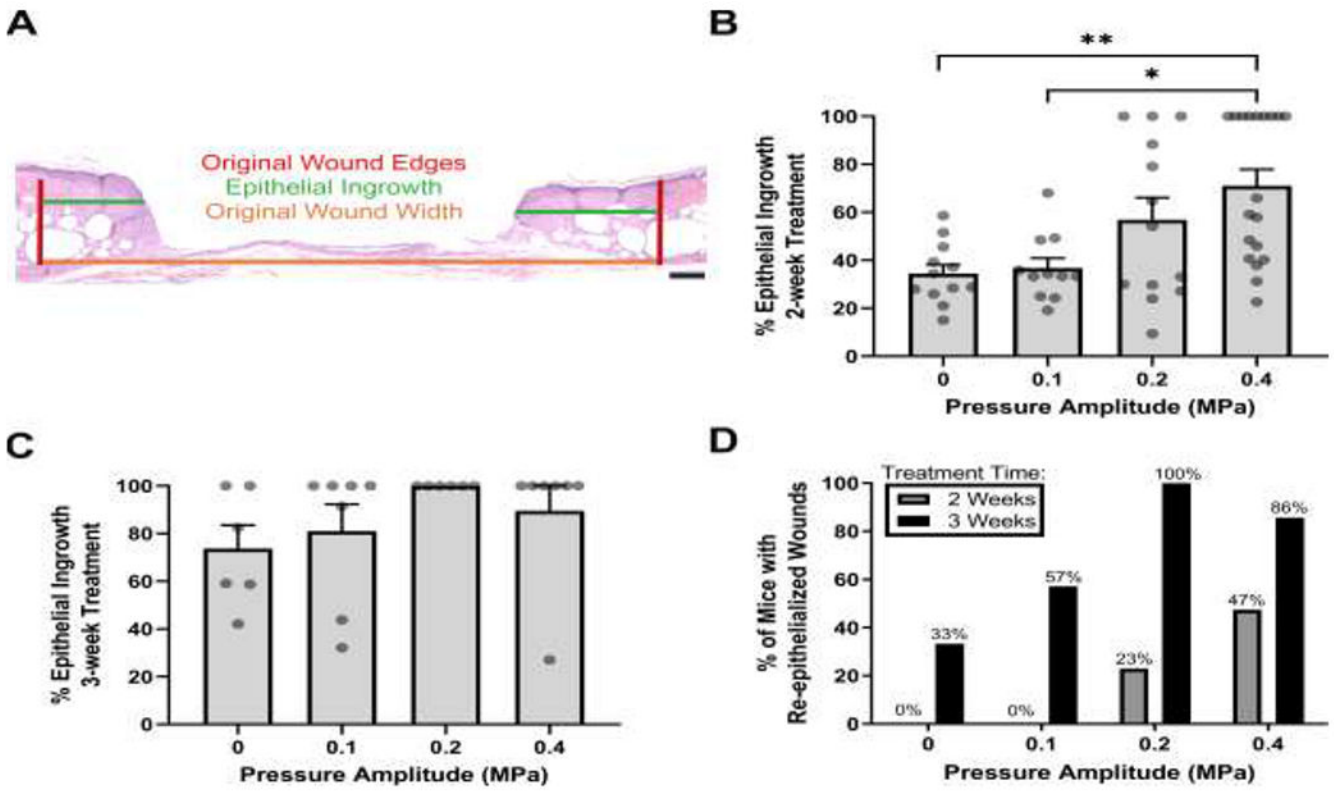

Fig. 6. Effects of ultrasound exposure on wound re-epithelialization

Tissue sections corresponding to wound centers were used to measure re-epithelialization after 2 or 3 weeks of ultrasound exposure. (A) Representative image of H&E-stained skin section illustrating measurements used to quantify re-epithelization. Shown are the original wound edges (red lines), epithelial ingrowth (green lines), and original wound width (orange line). Scale bar = 200 μm. Epithelial ingrowth was measured and reported as a percent of the original wound width at (B) 2 weeks (n = 11-19) and (C) 3 weeks (n = 6-7) after injury. Circles represent data from individual animals and bars indicate mean values (± SEM). Significance tested (*$p < 0.05$ and **$p < 0.01$) by Kruskal–Wallis test and Dunn's post-hoc test. Significant differences were found at 2 weeks between 0.4 MPa and both 0 MPa ($p = 0.006$) and 0.1 MPa ($p = 0.022$) conditions. (D) Measurements of epithelial ingrowth were used to calculate the percent of mice that had fully re-epithelialized wounds in each experimental group. Data are plotted as a function of pressure amplitude for 2-week (gray) and 3-week (black) exposures.

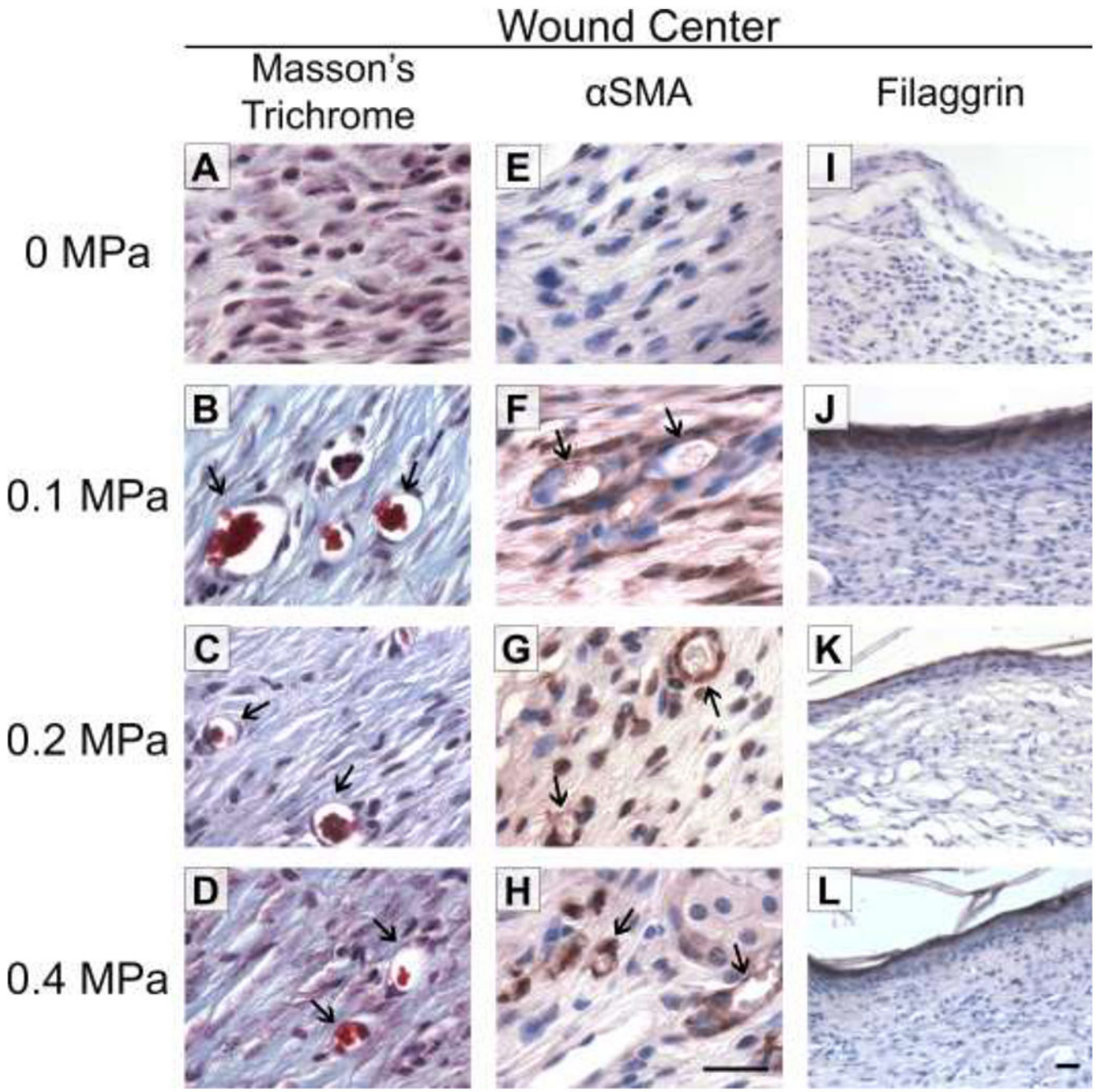

Fig. 7. Re-vascularization and epidermal maturation of ultrasound-exposed wounds

Full-thickness wounds were either sham-exposed (A, E, I) or exposed to 1-MHz ultrasound at pressure amplitudes of 0.1 MPa (B, F, J), 0.2 MPa (C, G, K), or 0.4 MPa (D, H, L) for 3 weeks. Tissue sections from wound centers were stained with Masson's trichrome (A-D) or anti-alpha-smooth muscle actin (αSMA) antibodies (E-H; brown staining) to visualize blood vessels (arrows). Scale bar = 25 αm. (I-L) Tissue sections from wound centers were stained with anti-filaggrin antibodies (brown). Scale bar = 25 αm.

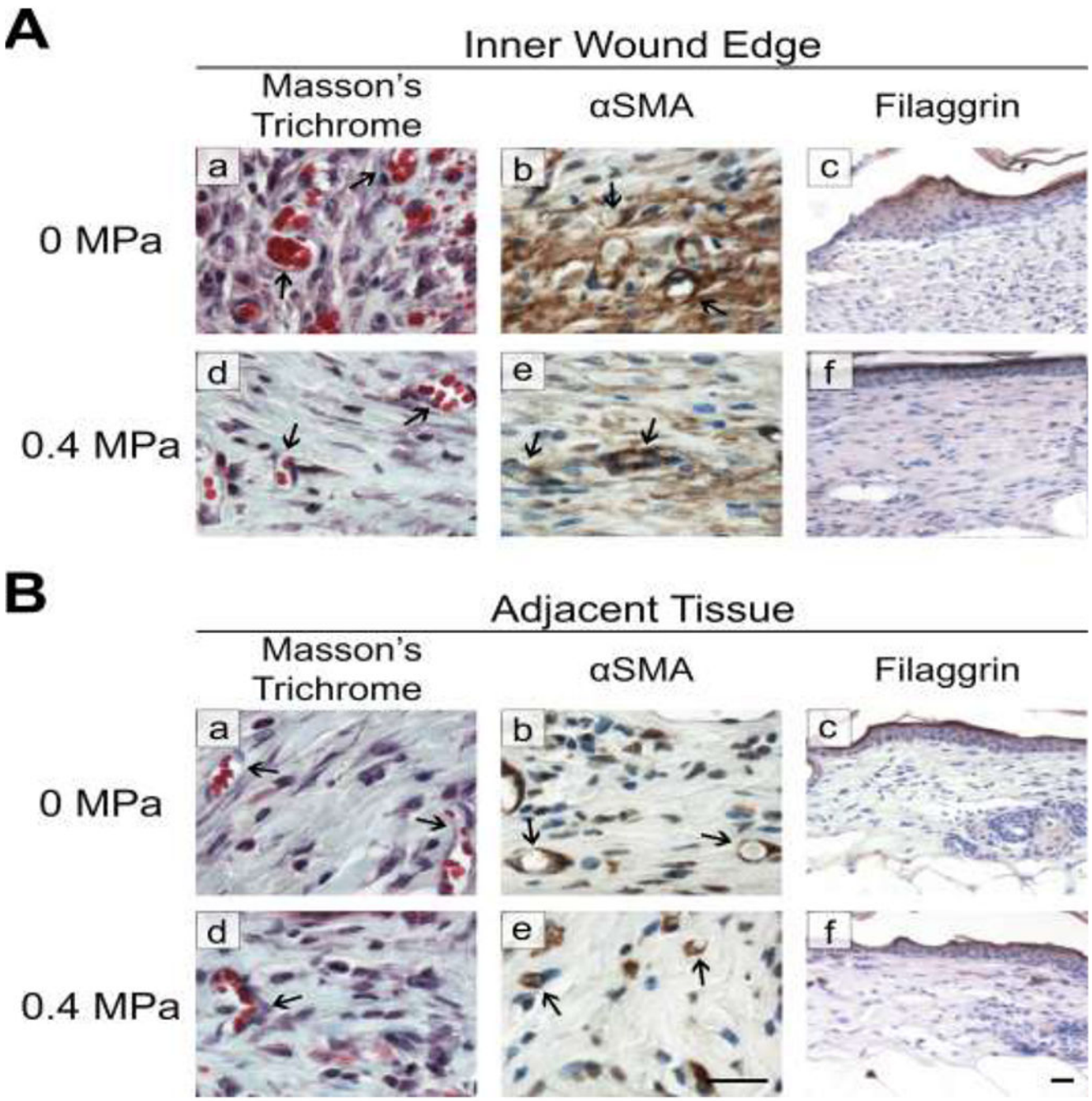

Fig. 8. Histological evaluation at the wound edge and in uninjured, adjacent tissue

Tissue sections obtained from mice that were exposed to either 0-MPa (sham) or 0.4-MPa ultrasound were evaluated (A) at the wound edge or (B) in uninjured skin adjacent to the wound. The presence of blood vessels (arrows) was evaluated using Masson's trichrome (a, d) or anti-α-smooth muscle actin antibodies (αSMA; b, e); anti-filaggrin antibodies were used to detect filaggrin (c, f). Scale bars = 25 αm